Chin. Ann. Math.
34B(3), 2013, 319–332
DOI: 10.1007/s11401-013-0775-y

Chinese Annals of Mathematics, Series B

A Pseudo-Kinetic Approach for Helmholtz Equation*

Radjesvarane ALEXANDRE[1] Jie LIAO[2]

Abstract A lattice Boltzmann type pseudo-kinetic model for a non-homogeneous Helmholtz equation is derived in this paper. Numerical results for some model problems show the robustness and efficiency of this lattice Boltzmann type pseudo-kinetic scheme. The computation at each site is determined only by local parameters, and can be easily adapted to solve multiple scattering problems with many scatterers or wave propagation in non-homogeneous medium without increasing the computational cost.

Keywords Lattice Boltzmann scheme, Non-homogeneous Helmholtz equation, Discrete velocity
2000 MR Subject Classification 35A05, 35B65, 35D10, 35H20, 76P05, 84C40

1 Introduction

Wave propagation and scattering problems arise from diverse application areas such as acoustics, aerodynamics, electromagnetics, antenna design, oceanography, etc. (see, e.g., [6, 14–15, 19]). We consider the non-homogeneous Helmholtz equation in frequency domain

$$\triangle A + k^2 n^2(\mathbf{x}) A = \phi(\mathbf{x}), \tag{1.1}$$

where $A = A(\mathbf{x})$ is the wave field at position $\mathbf{x} \in \mathbb{R}^N$, N is the dimension of space considered, $n(\mathbf{x}) = \frac{c_0}{c(\mathbf{x})}$ is the index of refraction, which is the ratio of the wave speed in the homogeneous background to that in the non-homogeneous medium or scatterers, $k = \frac{\omega}{c_0}$ is the wave number, ω is the wave frequency, and $\phi(\mathbf{x})$ on the right-hand side is the source function.

This problem has been intensively investigated, both numerically and analytically (see, e.g., [1, 9–10, 24–25, 28] and the references therein). However, the traditional computational methods for solving Helmholtz equation may suffer a very high cost for a reasonable big problem. With the development of GPGPU (general purpose computation on graphics processing units) devices and HPC (high performance computing) facilities, it deserves to design a massively parallel computing scheme to resolve this problem. For this purpose, we construct a pseudo-kinetic model for the non-homogeneous Helmholtz equation, which is a lattice Boltzmann (or

Manuscript received January 15, 2013.
[1]Department of Mathematics, Shanghai Jiao Tong University, Shanghai 200240, China; IRENAV Research Institute, French Naval Academy Brest-Lanvéoc 29290, France.
E-mail: radjesvarane.alexandre@ecole-navale.fr
[2]School of Science, East China University of Science and Technology, Shanghai 200237, China.
E-mail: liaojie@ecust.edu.cn
*Project supported by the National Natural Science Foundation of China (Nos. 11171211, 11171212) and the Fundamental Research Funds for the Central Universities.

LB for short) type scheme characterized by simple calculations, a massively parallel process among many other advantages (see [2]). For implementation of a lattice Boltzmann scheme on GPU (graphics processing units), see [20, 23, 29–30] and the references therein.

Before deriving our numerical scheme, we should make clear what is the solution to the non-homogeneous Helmholtz equation (1.1).

It is well-known that the solution to (1.1) in the whole space is non-unique in usual energy function space (see [7, 24, 27]). To ensure the uniqueness, we have to add for example the radiation condition at infinity. Instead, we shall shift to the following "damped" Helmholtz equation:

$$\triangle A + k^2(n^2(\mathbf{x}) + \mathrm{i}\epsilon)A = \phi(\mathbf{x}) \tag{1.2}$$

with $\epsilon > 0$ indicating the fraction of damping in the medium, which governs wave propagation in a barely attenuation medium. Here, in this paper, i denotes the imaginary unit. This damped equation has a unique solution in the space $H^2(\mathbb{R}^N)$ (see [7]). In [21–22], it is shown that the solution to (1.2) tends to the outgoing solution to (1.1) when ϵ goes to zero and that the obtained solution satisfies a new radiation condition (the limiting absorption principle). It is also shown there that the uniformly weighted L^2 and Morrey-Campanato-type estimates hold. In any case, since the solution to (1.2) in the whole space is unique and automatically outgoing, and due to the results of [21–22], we shall work on the damped Helmholtz equation (1.2) throughout this paper.

The radiation condition or the damped Helmholtz equation, however, is only satisfied in an infinite domain. For computational purposes, extending the domain to infinity is impractical. Therefore, we have to truncate the domain in such a way that a physically and computationally acceptable compromise is reached. An essential ingredient for this approach is to truncate an unbounded domain to a bounded domain by imposing an exact or approximate non-reflecting (absorbing or transparent) boundary condition (or NRBC for short) at the outer artificial boundary, where the NRBC is designed to prevent spurious wave reflection from the artificial boundary. In [16, 18], non-local boundary conditions are proposed to mimic the radiation condition at infinity. Despite their accuracy for any direction of wave incidence, the inclusion of this type of boundary condition in the discretization is impractical (and sometimes even false) because of the non-locality. Enquist and Majda in [8] proposed local boundary conditions for a truncated domain (see also [4–5]). Different types of local boundary conditions have also been proposed elsewhere (see, e.g., in [13, 11] and the references therein).

For this purpose, we utilize a local boundary condition fit for the kinetic scheme, through a change of the equilibrium profile function. In our scheme, we will introduce "attenuation nodes" (see [3]) near the artificial boundary, where the equilibrium state is required to attenuate with a multiplicative factor $\beta \in (0, 1)$. To mimic free propagation beyond the limits of the simulation, the solution is to gradually absorb the energy. This is achieved by surrounding the simulation lattice with some "sponge" layers of attenuation nodes. These layers are added around the physical domain whose functions are to damp out the incoming waves. Numerical simulations show a good agreement but we should point out that rigorous proofs of mathematical

convergence are still to be proven. We specialize to 2-dimensional space, but most of our results hold in 3-dimensional space though numerical simulations need to be performed.

The paper is organized as follows. In the next section, we will derive the pseudo-kinetic model for the (damped) non-homogeneous Helmholtz equation. This pseudo-kinetic model will then be discretized in Section 3, and numerical results for some model problems will be presented in Section 4. These numerical results will show the robustness and efficiency of this lattice Boltzmann type pseudo-kinetic scheme in application to multiple scattering problems with many scatterers or wave propagation in non-homogeneous medium.

2 Pseudo-Kinetic Model

Let us first mention that a time dependent kinetic wave model is a kinetic equation for the distribution of a continuum of particles by which the (damped) non-homogeneous Helmholtz equation is recovered. In the kinetic model, free movement is assumed for each fictitious particle. If the density of particles with velocity $\mathbf{v}$ at position $\mathbf{x}$ and time t is described by the function $\widetilde{f}(t,\mathbf{x},\mathbf{v})$, the evolution is given by the kinetic transport-collision process

$$\frac{\partial \widetilde{f}}{\partial t} + \mathbf{v}\cdot\nabla\widetilde{f} = L(\widetilde{f}) + \widetilde{S}(\mathbf{x},t)\delta(\mathbf{v}). \tag{2.1}$$

Here L is a linear collision operator (because we deal with a linear type Helmholtz equation) acting only w.r.t. to $\mathbf{x}$ and $\mathbf{v}$ variables, $\widetilde{S}$ is a source term, and δ is the Dirac delta function. Here and hereafter the operator ∇ is taken as the gradient of a function with respect to spacial variable $\mathbf{x}$. This first order linear transport equation is well-posed, and we understand the Dirac delta function $\delta(\mathbf{v})$ as a smooth axisymmetrical function with integration 1 over the velocity-space.

We assume a time harmonic form of the source term $\widetilde{S} = \mathrm{e}^{\mathrm{i}\omega t}S(\mathbf{x})$ in (2.1), where ω is the frequency, and consider time harmonic form distribution function

$$\widetilde{f}(t,\mathbf{x},\mathbf{v}) = \mathrm{e}^{\mathrm{i}\omega t}f(\mathbf{x},\mathbf{v}).$$

Then $L(\widetilde{f}) = L(f)\cdot\mathrm{e}^{\mathrm{i}\omega t}$, and the amplitude function $f(\mathbf{x},\mathbf{v})$ satisfies

$$\mathrm{i}\omega f + \mathbf{v}\cdot\nabla f = L(f) + S(\mathbf{x})\delta(\mathbf{v}). \tag{2.2}$$

There is no time variable in equation (2.2), and we shall thus call it a pseudo-kinetic equation. The linear collision operator L needs to be specified in this equation, and for simplicity we shall choose it to be given as a BGK type operator

$$L(f) = -\frac{1}{\tau}(f - M(f)),$$

in which τ is a single relaxation time, and the Maxwellian equilibrium $M(f)$ is a linear function of f to be specified.

To recover the Helmholtz equation from the pseudo-kinetic model (2.2), we define the associated macroscopic quantities

$$\int f\mathrm{d}\mathbf{v} = \rho, \quad \int f\mathbf{v}\mathrm{d}\mathbf{v} = \rho\mathbf{u}, \tag{2.3}$$

and define the local Maxwellian $M(f)$ as

$$M(f) = \Big(1 + \frac{1}{K}\mathbf{v}\cdot\mathbf{u}\Big)\frac{\rho}{(2K\pi)^{\frac{N}{2}}}\exp\Big(-\frac{|\mathbf{v}|^2}{2K}\Big), \tag{2.4}$$

where N is the dimension of space considered, and K will be chosen to yield the local wave velocity of a resulting Helmholtz equation. The local Maxwellian carries the macroscopic information (2.3) and furthermore satisfies

$$\int f|\mathbf{v}|^2 \mathrm{d}\mathbf{v} = NK\rho.$$

By using (2.3), we readily integrate (2.2) with respect to $\mathbf{v}$ to get

$$\mathrm{i}\omega\rho + \nabla\cdot(\rho\mathbf{u}) = S. \tag{2.5}$$

Similarly, the integration of (2.2) multiplied by $\mathbf{v}$ gives

$$\mathrm{i}\omega\rho\mathbf{u} + \nabla(K\rho) = 0, \tag{2.6}$$

then, from (2.5)–(2.6), we obtain

$$\omega^2\rho + \nabla^2(K\rho) = -\mathrm{i}\omega S. \tag{2.7}$$

To make precise the connection with our model wave problem (1.1), setting $A = K\rho$ and $\phi = -\mathrm{i}\omega S$, taking $K = c^2(\mathbf{x})$, using the notations above, we recover the non-homogeneous Helmholtz equation (1.1) from (2.7):

$$\triangle A + k^2 n^2(\mathbf{x})A = \phi(\mathbf{x}),$$

or, taking $K = \frac{c_0^2}{n^2(\mathbf{x})+\mathrm{i}\epsilon}$, we recover the damped non-homogeneous Helmholtz equation (1.2):

$$\triangle A + k^2(n^2(\mathbf{x}) + \mathrm{i}\epsilon)A = \phi(\mathbf{x}).$$

The conclusion is thus that we can solve the (damped) non-homogeneous Helmholtz equation by solving the pseudo-kinetic equation (2.2), since the macroscopic variable ρ, thus A, can be calculated from (2.3), once (2.2) is solved.

3 Computational Scheme

3.1 Lattice Boltzmann method

We use the standard 9-velocity lattice Boltzmann method (or LBM for short) with rectangular grid to discretize the pseudo-kinetic equation (2.2) in 2-dimensional case. The discrete velocities, $\mathbf{e}_\alpha$, $\alpha = 0, 1, \cdots, 8$, as shown in Figure 1, are given by

$$\begin{array}{l}\mathbf{e}_0 = (0,0), \quad \mathbf{e}_1 = (1,0), \quad \mathbf{e}_2 = (1,1), \quad \mathbf{e}_3 = (0,1), \quad \mathbf{e}_4 = (-1,1),\\ \mathbf{e}_5 = (-1,0), \quad \mathbf{e}_6 = (-1,-1), \quad \mathbf{e}_7 = (0,-1), \quad \mathbf{e}_8 = (1,-1).\end{array}$$

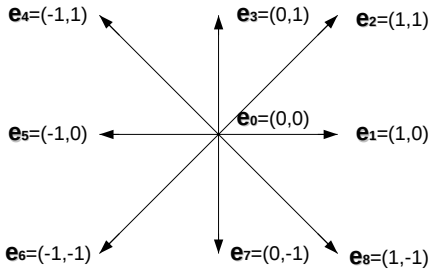

Figure 1 D2Q9 velocity components

Letting ε denote the lattice spacing, we propose the following lattice Boltzmann scheme:

$$\mathrm{e}^{\mathrm{i}\omega\varepsilon} f_i(\mathbf{x}+\varepsilon\mathbf{e}_i) = f_i(\mathbf{x}) - \frac{1}{\tau}(f_i(\mathbf{x}) - f_i^{\mathrm{eq}}(\mathbf{x})) + \Omega_i' \tag{3.1}$$

for $i = 0, 1, \cdots, 8$, where $f_i(\mathbf{x})$ is the local distribution function at site $\mathbf{x} = (x, y)$, with velocity $\mathbf{e}_i$, τ is a fixed relaxation parameter, Ω_i' is related to the source term, and the equilibrium function $f_i^{\mathrm{eq}}(\mathbf{x})$ will be specified later. Note that (3.1) is independent of time, so it is different from the traditional lattice Boltzmann equation. The lattice Boltzmann scheme (3.1) is determined once $f_i^{\mathrm{eq}}(\mathbf{x})$ and Ω_i' are specified, and by starting from proper initial condition, the distribution function $f_i(\mathbf{x})$ is marched synchronously to all lattice sites by an iterative procedure in a sort of pseudo-time (see [31–32]).

To recover the macroscopic variables, we define the wave height at site $\mathbf{x}$ as

$$\rho(\mathbf{x}) = \sum_{i=0}^{8} f_i(\mathbf{x}) \tag{3.2}$$

and the velocity field

$$\mathbf{u}(\mathbf{x}) = \frac{\sum\limits_{i=0}^{8} \mathbf{e}_i f_i(\mathbf{x})}{\sum\limits_{i=0}^{8} f_i(\mathbf{x})}. \tag{3.3}$$

The local equilibrium function $f_i^{\mathrm{eq}}(\mathbf{x})$ can be chosen as

$$f_i^{\mathrm{eq}}(\mathbf{x}) = \begin{cases} \Big(1 - \dfrac{5}{3}K\Big)\rho(\mathbf{x}), & i = 0, \\ \dfrac{1}{3}(K + \mathbf{e}_i \cdot \mathbf{u}(\mathbf{x}))\rho(\mathbf{x}), & i = 1, 3, 5, 7, \\ \dfrac{1}{12}(K + \mathbf{e}_i \cdot \mathbf{u}(\mathbf{x}))\rho(\mathbf{x}), & i = 2, 4, 6, 8, \end{cases} \tag{3.4}$$

which can be seen as an approximation to the Maxwellian equilibrium $M(f)$ defined in (2.4) (see, e.g., [17]). In particular, the basic constraints on the conservation of mass and momentum are satisfied, i.e.,

$$\sum_{i=0}^{8} f_i^{\mathrm{eq}}(\mathbf{x}) = \rho = \sum_{i=0}^{8} f_i(\mathbf{x}), \quad \sum_{i=0}^{8} \mathbf{e}_i f_i^{\mathrm{eq}}(\mathbf{x}) = \rho\mathbf{u} = \sum_{i=0}^{8} \mathbf{e}_i f_i(\mathbf{x}), \tag{3.5}$$

Note that now we have three important parameters in the lattice Boltzmann scheme (3.1): ε, K and τ, where ε characterizes the numerical accuracy of the scheme, τ is a relaxation parameter characterizing the stability and convergence of the lattice scheme (see [17]), and K is a parameter characterizing the local wave velocity as explained earlier. We will see in the next sub-section that this choice ultimately yields a limiting Helmholtz equation with local wave velocity $c(\mathbf{x}) = \sqrt{K}$.

3.2 Derivation of the Helmholtz equation

We consider $f_i(\mathbf{x})$ as a small perturbation about the local equilibrium $f_i^{\rm eq}(\mathbf{x})$, i.e.,

$$f_i(\mathbf{x}) = f_i^{\rm eq}(\mathbf{x}) + \varepsilon f_i^1(\mathbf{x}) + \varepsilon^2 f_i^2(\mathbf{x}) + \cdots, \tag{3.6}$$

and apply a standard Chapman-Enskog expansion (see [2, 26]). We rewrite LBE (3.1) as

$$\begin{aligned} &\mathrm{e}^{\mathrm{i}\omega\varepsilon}[f_i(\mathbf{x}+\varepsilon\mathbf{e}_i) - f_i(\mathbf{x})] + (\mathrm{e}^{\mathrm{i}\omega\varepsilon} - 1)f_i(\mathbf{x}) \\ &= -\frac{1}{\tau}(f_i(\mathbf{x}) - f_i^{\rm eq}(\mathbf{x})) + \Omega_i', \quad i = 0, 1, \cdots, 8, \end{aligned}$$

by performing the Taylor expansion, we obtain

$$\begin{aligned} &(1 + \mathrm{i}\omega\varepsilon + \cdots)\Big(\varepsilon\mathbf{e}_i \cdot \nabla f_i(\mathbf{x}) + \frac{(\varepsilon\mathbf{e}_i \cdot \nabla)^2}{2!} f_i(\mathbf{x}) + \cdots\Big) + (\mathrm{i}\omega\varepsilon + \cdots) f_i(\mathbf{x}) \\ &= -\frac{1}{\tau}(f_i(\mathbf{x}) - f_i^{\rm eq}(\mathbf{x})) + \Omega_i'. \end{aligned} \tag{3.7}$$

If we assume

$$\Omega_i' = \mathrm{i}\varepsilon\varphi, \tag{3.8}$$

then we can substitute (3.6) into (3.7), sum (3.7) over $i = 0, 1, \cdots, 8$ and equate coefficients of ε^1 to get

$$\nabla \cdot \Big(\sum_{i=0}^{8} \mathbf{e}_i f_i^{\rm eq}(\mathbf{x})\Big) + \mathrm{i}\omega\Big(\sum_{i=0}^{8} f_i^{\rm eq}(\mathbf{x})\Big) = 9\mathrm{i}\varphi.$$

By the constraints (3.5), we then have

$$\nabla \cdot (\rho(\mathbf{x})\mathbf{u}(\mathbf{x})) + \mathrm{i}\omega\rho(\mathbf{x}) = 9\mathrm{i}\varphi. \tag{3.9}$$

Next, we multiply (3.7) by $\mathbf{e}_i$ and sum over $i = 0, 1, \cdots, 8$, substitute $f_i(\mathbf{x})$ by (3.6) and again equate coefficients of ε^1. Noting that $\sum\limits_{i=0}^{8} \mathbf{e}_i\ \varphi = 0$, we readily have a pair of equations

$$\begin{aligned} &\frac{\partial}{\partial x}\Big(\sum_{i=0}^{8} e_{i\alpha}e_{ix} f_i^{\rm eq}(\mathbf{x})\Big) + \frac{\partial}{\partial y}\Big(\sum_{i=0}^{8} e_{i\alpha}e_{iy} f_i^{\rm eq}(\mathbf{x})\Big) \\ &+ \mathrm{i}\omega\Big(\sum_{i=0}^{8} e_{i\alpha} f_i^{\rm eq}(\mathbf{x})\Big) = 0, \quad \alpha \in \{x, y\}, \end{aligned}$$

where the right-hand side vanishes due to the conservation of momentum. This pair of equations can be rewritten as

$$\nabla \cdot \Pi^0(\mathbf{x}) + \mathrm{i}\omega\ \rho(\mathbf{x})\mathbf{u}(\mathbf{x}) = 0, \tag{3.10}$$

where Π^0 denotes the momentum tensor based on the local equilibrium f_i^{eq}. By using the explicit expression for $f_i^{\mathrm{eq}}(\mathbf{x})$ in (3.4), we notice that the momentum tensor is diagonal and the diagonal elements

$$\Pi^0_{xx} = \Pi^0_{yy} = K\rho(\mathbf{x}),$$

thus (3.10) can be simplified as

$$\nabla(K\rho(\mathbf{x})) + \mathrm{i}\omega\ \rho(\mathbf{x})\mathbf{u}(\mathbf{x}) = 0. \tag{3.11}$$

We further take the divergence of (3.11) and combine with (3.9) to get

$$\nabla^2(K\rho(\mathbf{x})) + \omega^2\rho(\mathbf{x}) = 9\varphi\omega.$$

Now again take

$$A(\mathbf{x}) = K\rho(\mathbf{x}),$$

then $A(\mathbf{x})$ solves

$$\Big(\nabla^2 + \frac{\omega^2}{K}\Big)A(\mathbf{x}) = 9\varphi\omega. \tag{3.12}$$

Next we set

$$K = c^2(\mathbf{x}), \quad \varphi = \frac{1}{9\omega}\phi$$

at each site, then we readily recover the non-homogeneous Helmholtz equation (1.1) from (3.12) again, or, we can just simply set

$$K = \frac{c_0^2}{n^2(\mathbf{x}) + \mathrm{i}\epsilon}, \quad \varphi = \frac{1}{9\omega}\phi \tag{3.13}$$

to recover the "damped" Helmholtz equation (1.2), where $n(\mathbf{x}) = \frac{c_0}{c(\mathbf{x})}$ is the index of reflection defined as before.

We should mention that we can not follow the multiscale approach from [17, 31] in the time dependent case, since in the harmonic case, time dependence has already been fixed.

4 Implementation and Numerical Results

Recall the lattice Boltzmann scheme (3.1):

$$\mathrm{e}^{\mathrm{i}\omega\varepsilon} f_i(\mathbf{x} + \varepsilon\mathbf{e}_i) = f_i(\mathbf{x}) - \frac{1}{\tau}(f_i(\mathbf{x}) - f_i^{\mathrm{eq}}(\mathbf{x})) + \Omega_i',$$

where $f_i^{\mathrm{eq}}(\mathbf{x})$ defined in (3.4) depends on K, and K is given by (3.13), the source term Ω_i' is given by (3.8). The computation strategy consists of the following steps:

Step 1 Initialization. We initialize all the microscopic distribution functions $f_i(\mathbf{x})$ to be 0;

Step 2 Iterate the distribution function by LB scheme (3.1);

Step 3 Update the macroscopic variables by (3.2)–(3.3) and calculate the equilibrium function $f_i^{\rm eq}(\mathbf{x})$ by (3.4);

Step 4 Repeat steps 2 and 3 until steady state is obtained.

Due to the advantages of the simple LBM scheme, the numerical simulation can be much simplified and easily parallelizable, compared with directly solving the Helmholtz equation by traditional computational methods.

4.1 Scales and parameters

For implementation of the lattice Boltzmann scheme, we should firstly set up suitable scales. The physical parameters in the scheme are the wave frequency ω, background wave speed c_0 and local wave speed $c(\mathbf{x})$. We use only two distinguished parameters, which are the wave number $k = \frac{\omega}{c_0}$ and the index of reflection $n(\mathbf{x}) = \frac{c_0}{c(\mathbf{x})}$, and rescale the wave frequency ω to be 1. This can be arrived by setting

$$\omega\varepsilon \to \widetilde{\varepsilon}, \quad \omega\mathbf{x} \to \widetilde{\mathbf{x}}, \quad f_i(\mathbf{x}) \to \widetilde{f}_i(\widetilde{\mathbf{x}}), \quad \text{etc.}$$

in (3.1) and omit the tilde to have

$$\mathrm{e}^{\mathrm{i}\varepsilon} f_i(\mathbf{x} + \varepsilon\mathbf{e}_i) = f_i(\mathbf{x}) - \frac{1}{\tau}(f_i(\mathbf{x}) - f_i^{\rm eq}(\mathbf{x})) + \Omega_i'. \tag{4.1}$$

The spacial and pseudo-temporal parameters are the lattice spacing ε and relaxation parameter τ. The stability condition for LBM model requires $\tau > 0.5$ (see, e.g., [12]).

Now we consider the new equation (4.1) in the rescaled computation domain. The computation domain will be chosen as a square $[-5, 5]^2$ in the following computations. We use $N = 235$ grid points in each spacial direction thus the lattice size $\varepsilon = \frac{10}{N} \approx 0.0426$. By taking a wave number $k = 5$, the wave length $\lambda = \frac{2\pi}{k} \approx 1.2566$, and thus we have about 30 grid points per wave (or ppw for short).

4.2 Boundary treatment

As discussed above, to approximate the non-reflecting (absorbing or transparent) boundary condition (or NRBC for short) on the computation domain, we use "attenuation nodes" near the artificial boundary (see [3]), where the equilibrium state is modified as follows: We attenuate it by a smooth multiplicative factor $\beta \in (0, 1)$ which grows gradually from 0 on the artificial boundary to 1 on the boundary of the square. The attenuation nodes act as a "sponge" layer, whose function is to damp out the incoming waves. In our simulations, we take 10 additional points around the square as attenuation nodes. Spurious numerical reflection at the boundary does almost not present due to the boundary treatment.

4.3 Numerical results

For evaluation of the numerical performance of the scheme proposed in the present work, we carry out numerical simulations on the following model problems. The model problems

represent an increasing level of difficulty which is suitable to test the robustness and efficiency of the lattice Boltzmann methods proposed in this paper.

Example 4.1 Wave propagation in homogeneous media. We take $k = 5$, $n(\mathbf{x}) \equiv 1$ and $\phi(\mathbf{x}) = \delta(\mathbf{x})$ in (1.1), where $\delta(\mathbf{x})$ is the Dirac delta function. The computation domain is a square $[-5, 5]^2$. We use $N = 235$ grids in each spacial direction and 10 attenuation grids around the square, thus lattice size $\varepsilon = \frac{10}{N}$. We approximate the Dirac delta source by

$$\delta_\alpha(\mathbf{x}) \approx \frac{1}{\pi\alpha^2} \exp\Big(-\frac{|\mathbf{x}|^2}{\alpha^2}\Big),$$

and take $\alpha = 2\varepsilon$ in this case. We consider non attenuate background thus the attenuation factor $\epsilon = 0$. The relaxation parameter $\tau = 0.6$ is chosen. The real part of the wave field is shown in Figure 2. It is a radial wave as a function of distance from the source.

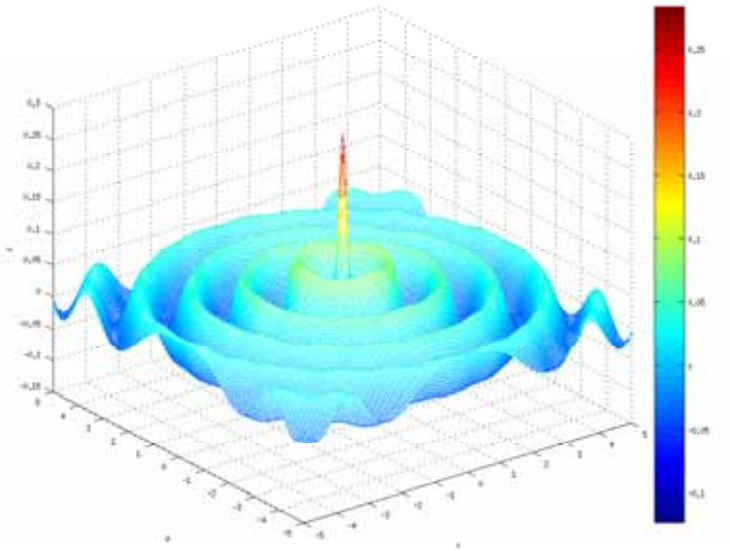

Figure 2 (Example 4.1) Mesh of the real part of numerical solution

It is well-known that the Green's function for the model problem is

$$G(\mathbf{x}) = \frac{\mathrm{i}}{4} H_0^{(1)}(k\mathbf{x}),$$

where $H_0^{(1)}$ is the first kind Hankel function of order 0. If we take the radial wave as a function of distance from the source, the comparison of the wave with the Green's function is shown in Figure 3.

As can be seen, there is a very good match between the wave shape and the Green's function, the numerical error near the source is induced by the nature of the singularity of the Dirac delta function, and the wave near the boundary is a little bit weaker than expected mostly due to the absorption boundary conditions used. Spurious numerical reflection is hardly seen due to the boundary treatment.

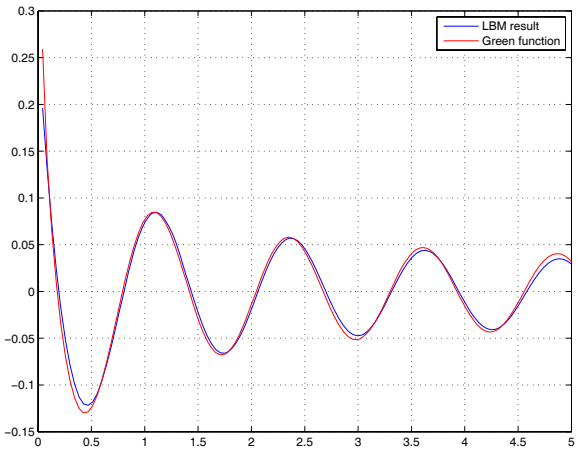

Figure 3 (Example 4.1) The comparison of the wave with the Green's function

Example 4.2 We consider the similar problem as Example 4.1 but with two point sources located at $(\pm 1.2, 0)$. The contour and mesh of the real part of numerical solution are shown in Figure 4(a) and Figure 4(b). As shown in the numerical results, we can see the "superposition" wave pattern of the waves emitted from two point sources.

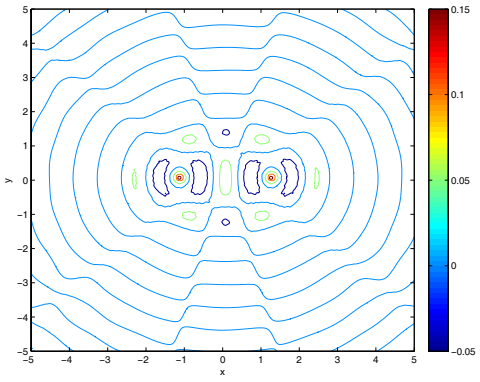

(a) Contour of the real part of numerical solution

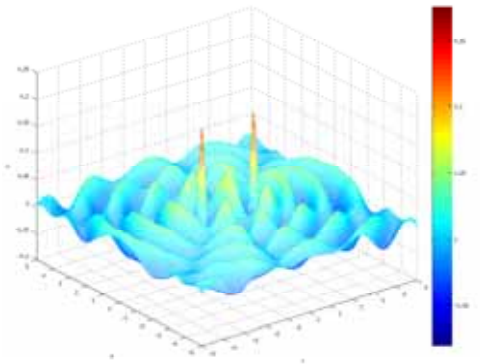

(b) Mesh of the real part of numerical solution

Figure 4 (Example 4.2) Two point sources located at $(\pm 1.2, 0)$

To show the application of the LB scheme to multiple scattering problem with many scatterers or wave propagation in non-homogeneous medium, we consider the next two models problems.

Example 4.3 Scattering of wave emitted from one source by 3 scatterers. In this example, we set up the same computation domain as in Example 4.1 above, consider one point source located at $(-2, 0)$ and three point scatterers located at $(2, \pm 2)$ and $(4, 0)$. The reflection index of each scatterer is taken as $n = 5$. Other parameters are the same as in Example 4.1. The total wave (wave incident by the source and wave scattered from the scatterers), the incident wave

and the scattered wave are plotted in Figure 5. The result clearly shows the weak scattering from each scatterer. This example can be easily extended to scattering problem with many scatterers without increasing the computational cost, since the parallel nature of the LB scheme let our computation at each site proceed simultaneously and use only the local parameter (reflection index).

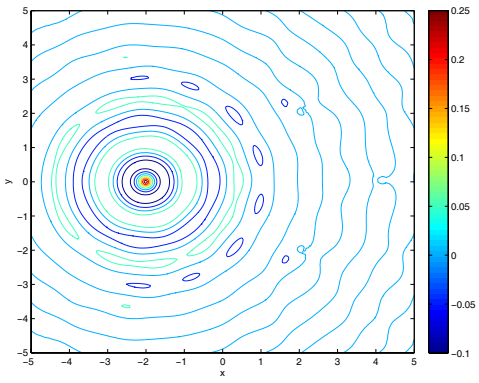

(c) Real part of the total wave

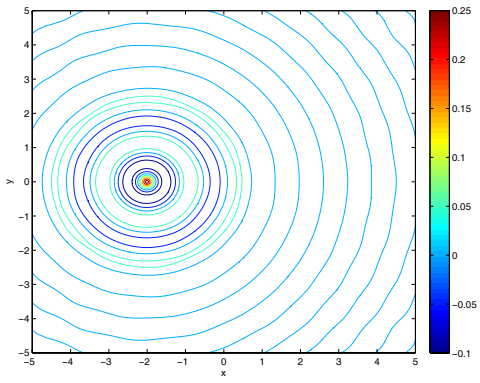

(d) Real part of the incident wave

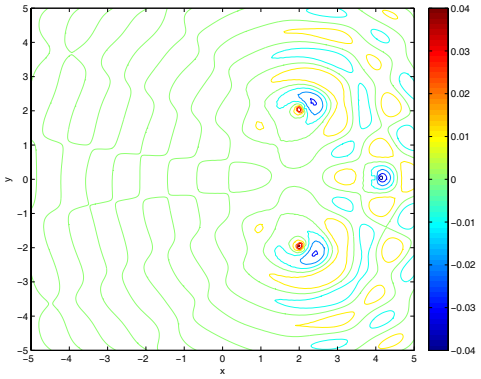

(e) Real part of the scattered wave

Figure 5 (Example 4.3) Scattering of wave emitted from one source by 3 scatterers

Example 4.4 Scattering of wave emitted from one point source by non-homogeneous medium. We set up the same computation domain as in Example 4.1 above, consider the medium with refraction index $n = 5$ or $n = 0.5$ in the right half of the computation domain, i.e.,

$$n(\mathbf{x}) = 1, \quad \text{in } [-5, 0] \times [-5, 5], \quad n(\mathbf{x}) = 5 \text{ or } 0.5, \quad \text{in } [0, 5] \times [-5, 5].$$

The location of the source is $(-2, 0)$ as in Example 4.3. The real part of numerical solutions will be shown in Figures 6 and 7.

From Figure 6, we see that for $n = 0.5$ case, where local wave speed is twice of the wave speed in the background, thus the wave travels more easily into non-homogeneous medium, but

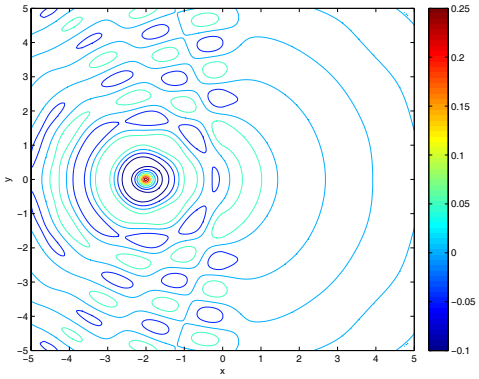

(f) Real part of the total wave

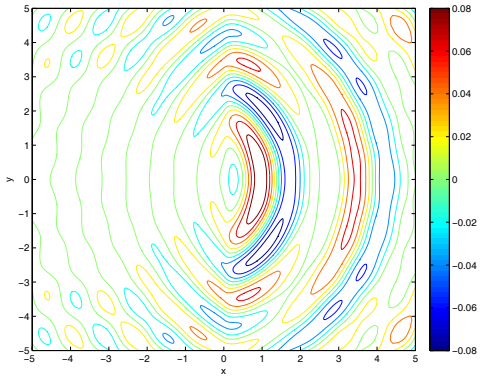

(g) Real part of the scattered wave

Figure 6 (Example 4.4) n=0.5 in the right half domain

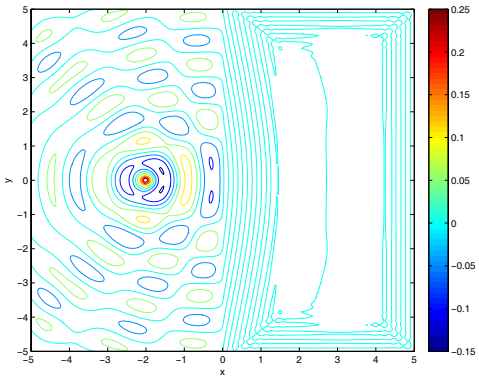

(h) Real part of the total wave

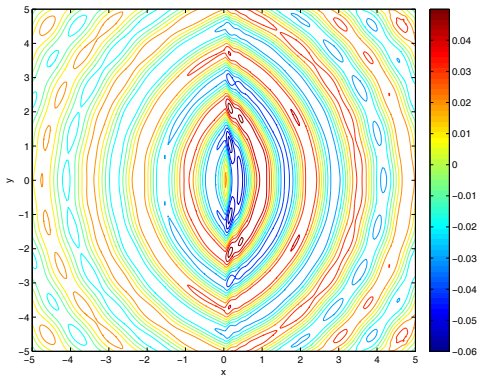

(i) Real part of the scattered wave

Figure 7 (Example 4.4) n=5 in the right half domain

for $n = 5$ case, the wave travels more slowly in the inhomogeneity. Both figures in Figure 6(g) and Figure 7(i) give the clear wave pattern of the scattered wave, which reveal the reflected wave in the left half domain and the refracted wave in the right one.

4.4 Conclusion and further difficulties

The above results on a series of model problems with an increasing level of difficulty showed the robustness and efficiency on solving time harmonic wave scattering problems by the lattice Boltzmann type scheme. However, the theoretical analysis remains to be done: One point is related to the fact that the usual multiscale Chapman-Enskog expansion can not be applied due to the time harmonic constraint; another point is related to the justification of the "damped" equilibrium function in precisely simulating an absorbing type condition. A further difficulty of this scheme is application to high frequency waves.

References

[1] Bayliss, A., Goldstein, C. I. and Turkel, E., An iterative method for the Helmholtz equation, *J. Comput. Phys.*, **49**, 1983, 443–457.

[2] Benzi, R., Succi, S. and Vergassola, M., The lattice Boltzmann equations: theory and applications, *Phys. Rep.*, **222**, 1992, 147–197.

[3] Chopard, B., Luthi, P. O. and Wagen, J. F., Lattice Boltzmann method for wave propagation in urban microcells, *IEEE Proc. Microw. Antennas Propag.*, **144**(4), 1997, 251–255.

[4] Clayton, R. and Engquist, B., Absorbing boundary conditions for acoustic and elastic wave equations, *Bull. Seis. Soc. America*, **67**(6), 1977, 1529–1540.

[5] Clayton, R. and Engquist, B., Absorbing boundary conditions for wave-equation migration, *Geophysics*, **45**(5), 1980, 895–904.

[6] Collins, M. D. and Kuperman, W. A., Inverse problems in ocean acoustics, *Inverse Problems*, **10**, 1994, 1023–1040.

[7] Egorov, Y. V. and Shubin, M. A., Foundations of the Classical Theory of Partial Differential Equations (Translated by R. Cooke), Encyclopaedia of Mathematical Sciences, Vol. 30, Springer-Verlag, New York, 2001.

[8] Engquist, B. and Majda, A., Absorbing boundary conditions for the numerical simulation of waves, *Math. Comput.*, **31**, 1977, 629–651.

[9] Fries, T. P. and Belytschko, T., The extended/generalized finite element method: An overview of the method and its applications, *Int. J. Numer. Meth. Engng*, **84**, 2010, 253–304.

[10] Giladi, E. and Keller, J. B., A hybrid numerical asymptotic method for scattering problems, *J. Comput. Phys.*, **174**, 2001, 226–247.

[11] Givoli, D. and Patlashenko, I., Optimal local non-reflecting boundary conditions, *Appl. Numer. Math.*, **27**, 1998, 367–384.

[12] He, X. and Luo, L. S., Theory of the lattice Boltzmann method: From the Boltzmann equation to the lattice Boltzmann equation, *Phys. Rev. E*, **56**, 1997, 6811–6817.

[13] Higdon, R. L., Numerical absorbing boundary conditions for the wave equation, *Math. Comp.*, **49**(179), 1987, 65–90.

[14] Ishimaru, A., Theory and application of wave propagation and scattering in random media, *Proceedings of the IEEE*, **65**, 1977, 1030–1061.

[15] Ishimaru, A., Wave Propagation and Scattering in Random Media, Series on Electromagnetic Wave Theory, IEEE Press, New York, 1997.

[16] Lindman, E. L., Free space boundary conditions for time dependent wave equation, *J. Comput. Phys.*, **18**, 1975, 66–78.

[17] Luthi, P. O., Lattice Wave Automata: From Radio Waves to Fractures Propagation, Phd Thesis, Universite de Geneve, 1997.

[18] Majda, A. and Osher, S., Reflection of singularities at the boundary, *Comm. Pure Appl. Math.*, **28**, 1975, 277–298.

[19] Martin, P. A., Multiple Scattering: Interaction of Time-Harmonic Waves with N Obstacles, Encyclopedia of Mathematics and its Applications, Vol. 107, Cambridge University Press, Cambridge, 2006.

[20] Obrecht, C. and Kuznik, F., Tourancheau, B. and Roux, J., Multi-GPU implementation of the lattice Boltzmann method, *Comp. Math. Appl.*, **65**(2), 2013, 252–261.

[21] Perthame, B., Vega, L., Energy concentration and Sommerfeld condition for Helmholtz and Liouville equations, *C. R. Acad. Sci. Paris, Ser. I*, **337**, 2003, 587–592.

[22] Perthame, B. and Vega, L., Morrey-Campanato estimates for Helmholtz equations, *J. Funct. Anal.*, **164**, 1999, 340–355.

[23] Riegel, E., Indinger, T. and Adams, N. A., Implementation of a lattice Boltzmann method for numerical fluid mechanics using the nVIDIA CUDA technology, *Computer Science-Research and Development*, **23**, 2009, 241–247.

[24] Sommerfeld, A., Partial Differential Equations in Physics, Academic Press, New York, 1964.

[25] Strouboulis, T., Babuskab, I. and Hidajat, R., The generalized finite element method for Helmholtz equation: Theory, computation, and open problems, *Computer Methods in Applied Mechanics and Engineering*, **195**, 2006, 4711–4731.

[26] Succi, S., The Lattice Boltzmann Equation for Fluid Dynamics and Beyond, Oxford University Press, Oxford, 2001.

[27] Taylor, M. E., Partial differential equations II: Qualitative studies of linear equations, Applied Mathematical Sciences, Vol. 116, Springer-Verlag, New York, 1996.

[28] Tikhonov, A. N. and Samarskii, A. A., Equations of Mathematical Physics, Dover Publ., New York, 1990.

[29] Tolke, J., Implementation of a lattice Boltzmann kernel using the compute unified device architecture developed by nVIDIA, *Comput. Visual. Sci.*, **13**, 2010, 29–39.

[30] Tubbs, K. and Tsai, F., GPU accelerated lattice Boltzmann model for shallow water flow and mass transport, *Int. J. Numer. Meth. Engng.*, **86**, 2011, 316–334.

[31] Yan, G., A lattice Boltzmann equation for waves, *J. Comput. Phys.*, **161**, 2000, 61–69.

[32] Zhang, J., Yan, G. and Dong, Y., A new lattice Boltzmann model for the Laplace equation, *Appl. Math. Comput.*, **215**, 2009, 539–547.